NARAM 56 (2014)

Research and Development

Team Division

Optimizing Piston Configuration For FAI Events S3A, S6A, and S9A

T-859

"Neutron Fusion"

Neutron Fusion, Team # 859:

Patrick Peterson

Chan Stevens

George Gassaway

Ed LaCroix

Terrill Willard

Patrick Peterson performed all static tests, data analyses, interpretation, and writing (July 2014) in consultation with the other members of the Neutron Fusion team.

Special acknowledgement is due to Trip Barber and Steve Krystal who provided the original motivation for this project, suggesting that the US Team might benefit by applying the concept of piston-adjusted thrust to the optimization of pistons for FAI competition. We would also like to thank Keith Vinyard, Tim Van Milligan, and George Gassaway who provided 10mm motors for this research.

Optimizing Piston Configuration For FAI Events S3A, S6A and S9A

Table of Contents

Optimizing Piston Configuration for FAI Events S3A, S6A, and S9A

(Neutron Fusion, Team # 859: NARAM-56 R&D report)

(1) 300-Word Summary

Our NARAM-55 (2013) R&D report introduced the concept of piston-adjusted thrust, showing how static test data of motor/piston configurations essentially "re-draw" the motor's thrust-time curve. This method allows us to determine for each point on the piston-adjusted thrust curve the velocity and position of the piston. From a single static test with a sufficiently long piston tube, we can determine the optimal sub-length with respect to the motor, liftoff weight, piston diameter, and initial piston volume used in the test.

While the NARAM-55 study considered C6 motors firing against 153g, in the current study we applied the concept of piston-adjusted thrust to 10mm and 13mm A motors, testing 28g liftoff weights representative of FAI competition events S3A, S6A, and S9A. We improved the method of static testing by measuring piston-adjusted thrust with a load cell, allowing for more precise measurement within the shorter duration of piston travel typical of A motors. We derived new formulas for acceleration and length of travel as a function of piston-adjusted thrust.

We performed static tests with and without pistons for three types of motors: the Serbian "Ultra" A2, the Apogee A2, and the Estes A3. Optimal piston configuration was defined as the length, diameter, and initial volume providing the largest increase in impulse over that of the motor without a piston. Our objective was to identify for these motors the optimal piston configuration(s) relative to a 28g weight. Results show that the A3 motor is optimized using zero-volume 86cm pistons with 10mm diameter, while both A2 motors were optimized using zero-volume 172cm pistons with 10mm diameter. These results are surprising: To our knowledge, the 10mm diameter has never been used for the A3, and pistons ≥ 86cm were not previously considered beneficial for such a low liftoff weight.

(2) Objectives of this Study

Optimal piston configuration was defined as the length, diameter, and initial volume providing the largest increase in impulse over that of the motor without a piston. Our objective was to identify the optimal piston configuration(s) when firing A3 or A2 motors against a 28.3g movable piston (i.e. a 28.3g liftoff weight).

As in any study of optimality, our results were limited to the parameters and range over which we tested motors and pistons. So the optimal length of piston travel was defined as the best length under the maximum we tested (171cm). Optimal initial volume was defined as the best volume ≤ 8 cubic cm. Optimal piston diameter was defined as the better of either 10mm or 13mm diameter. Where we refer in this report to "optimal piston configuration," we mean the optimal piston within these constraints.

For each of the 3 types of motor tested (the "Ultra" A2, the Apogee A2, and the Estes A3), we chose to test only a set of motors with matching dates or lot numbers as a means of limiting the extent of between-motor variation. All thrust curves and the derived impulses were collected from our own static test data using the same load cell under the same method of calibration (See Sections 4 and 5 for details on methods).

The Serbian-made Ultra A2 motors are currently popular for FAI competitions, partly because of their small size and weight. This is a 10mm motor with a thrust curve similar to the 10mm, US-made Apogee A2 (which is no longer commercially available nor NAR certified). For this study, we had available a limited number of the Ultra and Apogee A2 motors for static testing. The Apogee motors are still potentially relevant because of their similarity to the Ultra motors, and also because FAI use of these motors (from private stocks) may still be an option.

To our knowledge, the 13mm Estes A3 motor is not commonly used in FAI competition. However, some US team members have expressed an interest in using the A3 for events such as S3A (A Parachute Duration), S6A (A Streamer Duration), and S9A (A Gyrocopter Duration), as this would allow for greater consistency between practice flying and the actual FAI competition flying, where limits on the availability of European-made motors tend to hamper efforts to test and practice prior to competition. The A3 is widely used as a practice motor prior to FAI competitions, so even if it is not used directly in competition, it's inclusion in the current study is relevant and appropriate.

In addition, inclusion of the A3 allowed us to perform more controlled static tests than would have otherwise been possible (given the limited availability of A2 motors with matching dates). So for example, we performed a number of tests of non-zero initial volumes using the A3, to get a sense of whether it was even worth considering non-zero volumes for the A2 motors.

Although not a direct objective of this study, study results for the Estes A3 motor will also be applicable to many NAR competition events.

Liftoff weights for FAI events S3A, S6A, and S9A can vary by construction materials, recovery device, motor, and piston. However, the weight range for S3A, S6A, and S9A (including the possibility of adding a very long piston to the liftoff weight) is most likely between 20g and 40g. We chose to conduct the current study tests and analyses at 28.3g (1 ounce), considering that this is a familiar reference weight in English units, but also close to the midpoint of this range of liftoff weight for these events.

We believe any results obtained for 28.3g will be applicable to any model with liftoff weight roughly between 16g and 40g. A ±12g change in the net force should be negligible, about a 0.01N-sec change in the net impulse during piston travel typically lasting only a tenth of a second. Also, it appears that the pattern (not necessarily the magnitude) of how the thrust curve changes over the duration of piston travel is what most dictates which piston configuration is optimal. The fact that weight has a constant effect on the net force, and the fact that 12g represents only a very small change in the net force, lead us to believe that the optimal piston configuration(s) will not be substantially affected by weight changes of this magnitude.

For piston tube length in the static tests, we used 34-inch (86cm) Kraft paper tubes from Balsa Machining Service. Tests involved either a single tube (roughly 85cm of travel with zero initial volume) or two of these tubes connected with an external coupler (roughly 171cm of travel with zero initial volume). These test lengths would allow us to evaluate and assess the optimal length of piston travel across a nearly continuous range of values less than or equal to either maximum (see Section 4 for more details on the analytic methods). These paper tubes are very similar (or even identical) to typical piston tubes used by the US Team in FAI competition.

(3) Previous Related Work

The Barber Team's NARAM-14 R&D report, "The Dynamics of the Closed-Breech Launcher" described the basic mathematics of the motion of a rocket on a piston launcher. Geoff Landis' NARAM-17 report, "An Investigation of the Physics of the Zero Volume Piston Launcher" further developed the mathematical model.

At NARAM-16, the R&D report, "Optimization of the Zero Volume Piston Launcher" by Robert Thoelen, Thomas Bauer, and Paul Porzio included data from 152 test flights comparing different lengths of piston tubes for fixed-head, zero-volume launchers. Test models weighed between 30 and 40 grams, using pistons of lengths 6 inches to 18 inches. Among the motors tested were Estes 1/2A6 and A8 motors, with observed improvements in altitude as compared to flights off a launch rod. However, they did not see substantial differences in altitude relative to different piston lengths.

The Crunch Birds team compared 9-inch and 18-inch 13mm pistons, as described in their NARAM-30 report, "Empirical Evaluation of Optimum Piston Tube Length for a Floating Head Piston Launcher". They concluded that 18-inch tubes did not increase exit velocity over the 9-inch tubes.

These latter two reports suggest that for lightweight models and low-powered motors, very small lengths of piston tube may be optimal. However, Jonathan Dunbar's NARAM-53 report, "Determination of Optimum Piston Length for 13mm motors" found superior altitudes with 1/2A3 motors flown using 24-inch pistons, as compared to 12-inch, 15-inch, and 18-inch pistons.

A presumption is often made that pistons will continuously improve performance up to some maximum length, at which either there is a waning of piston pressure or the weight of any longer piston will detract from performance. However, additional results in Dunbar's report suggest this "conventional wisdom" may be wrong. The 15-inch pistons actually performed worse than both 12-inch and 18-inch pistons, which performed similarly. So although Jonathan ultimately saw superior performance at 24 inches, there wasn't any linear increase in performance at the smaller lengths. This suggests that piston pressure may ebb and flow during piston travel. Optimization may

mean identifying the pattern of waxing and waning thrust and choosing a “sweet spot” (say, following a particularly big wave of thrust) as the ideal moment for separation. This hypothesis is further supported by Landis’ NARAM-17 R&D report that identified patterns of waxing and waning thrust in the pistons he tested. Landis also simulated piston launches in a computer program, and these simulations predicted patterns of increasing and decreasing thrust. Our team’s NARAM-55 R&D report, “The Effect of Piston Launchers on Thrust-Time Curves,” specifically hypothesized patterns of waxing/waning thrust within a piston --- and this was indeed confirmed by the study’s experimental data. Both Landis and our team found that the use of zero initial volume was more strongly associated with problematically large drops in thrust, as compared to non-zero initial volumes.

Our team further speculated that zero volume could be sub-optimal, at least for some motors and liftoff weights. Under this theory, when using zero volume with certain motors and sufficiently high liftoff weight, there is extreme pressure initially built up close to and within the motor’s nozzle. This leads to a kind of initial “big bang” of first piston motion, after which thrust quickly drops (possibly because the volume has expanded more rapidly than the motor’s ability to fill that volume). This may set in motion a cycle whereby pressure builds, volume expands, pressure drops, pressure builds again, volume expands, etc. --- continuing for perhaps many cycles. We speculated that at least to some degree, cycles of rising and falling pressure may be an inherent characteristic of all piston launchers (assuming pistons of sufficient length in which to realize multiple cycles). For a given motor and liftoff weight, a key question is whether some initial non-zero volume can dampen the extreme swings of these cycles in a way that results in greater impulse.

Our team’s NARAM-55 (2013) R&D report is notable for several additional reasons. This report introduced a mathematical definition of piston-adjusted thrust (described in Section 4 of the current report), appropriately comparable to the NAR S&T concept of motor thrust, so as to allow for direct comparison of a piston-adjusted thrust-time curve with the corresponding motor thrust-time curve. The report also described a method of static testing for measuring piston-adjusted thrust over time, applicable to all conventional piston-launcher designs, and in principle able to measure the

effect of piston length to any maximum (for a given weight , diameter, and initial volume). More specifically, this method allows for determining for each point on the piston-adjusted thrust curve the velocity and position of the piston. So a single static test of a sufficiently long piston tube can determine the exact sub-length that optimized impulse for that tested motor, liftoff weight, piston diameter, and initial piston volume. Using this approach, this study was the first to provide quantitative proof that a piston launcher can add impulse to a motor's rated impulse. It was the first to demonstrate improved piston performance using a small non-zero initial volume, compared to zero volume (for C6 motors against a 153g liftoff weight). And finally, this was the first study to show that a piston more than 86cm long can out-perform shorter pistons.

(4) Analytic Methodology of the Current Study

As mentioned in Section 3, the early development of a mathematical model of rocket motion on a piston launcher was due primarily to Trip Barber and Geoff Landis. They applied Newton's second law of motion to derive the following equation:

$$(9.82\ m/sec^2)^{-1}\ W(t)\ a(t) \ = \ T(t) + [P(t) - P_A(t)]\pi r^2 - W(t) - D_{Aero}(t) - D_{Fric}(t),$$

where r is the radius of the piston tube, a(t) is the acceleration of the piston at time t, T(t) is the motor's thrust inside the piston at time t, P(t) is the pressure from exhaust gas at time t, $P_A(t)$ is the ambient atmospheric pressure at time t, W(t) is the sum of opposing weights at time t, $D_{Aero}(t)$ is the sum of aerodynamic drag at time t, and $D_{Fric}(t)$ is the drag due to friction on the piston at time t.

Our team's NARAM-55 R&D entry defined "piston-adjusted thrust" in a way that closely parallels how thrust over time is conventionally measured for rocket motors. A motor's thrust-time curve --- denoted in this report by M(t) --- is independent of both liftoff weight and aerodynamic drag: the liftoff weight and the aerodynamic drag are not subtracted from M(t). Therefore, we similarly defined the piston-adjusted thrust-time curve --- denoted by F(t) --- without subtracting the liftoff weight and aerodynamic drag: F(t) is defined as the upward force at time t due to the motor and the piston, minus the opposing force at time t due to atmospheric pressure and friction:

$$F(t) = T(t) + [P(t) - P_A(t)]\pi r^2 - D_{Fric}(t).$$

Assuming this definition, the Barber/Landis equation can be written as:

$$(9.82\ m/sec^2)^{-1}\ W(t)a(t) \ = \ F(t) - W(t) - D_{Aero}(t).$$

In this version of the Barber/Landis equation, W(t) represents the combined weight of the fully prepped rocket, motor, and piston tube at time t. Small changes in weight over the duration of piston travel can occur due to the motor's burn, and also because of gas leaks in the piston. However, because of the brief duration of piston travel, the effect of these weight changes should be negligible. So we ignored these small variations in weight and replaced the term W(t) with a fixed quantity W, representing the liftoff

weight. Therefore, rewriting the Barber/Landis equation for piston motion in terms of the piston-adjusted thrust F(t), we have:

$$F(t) = (9.82\ m/sec^2)^{-1}\ W\ a(t) + W + D_{Aero}(t).$$

For our team's NARAM-55 R&D report, static tests were set up with a fixed motor firing upward inside a fixed clear plastic tube, against a movable piston head of weight W. Velocity of the piston head upward was measured visually from high-speed video, with the acceleration derived at several points in time from the measured velocities. For this type of static test, the acceleration and the aerodynamic drag could theoretically differ from an actual piston launch of a rocket, so we write the equation of motion as:

$$F^*(t) = (9.82\ m/sec^2)^{-1}\ W\ a^*(t) + W + D^*_{Aero}(t),$$

where $a^*(t)$ and $D^*_{Aero}(t)$ represent the acceleration and aerodynamic drag specific to the static test. So $F^*(t)$ denotes the piston-adjusted thrust specific to the static test.

Assuming equal weight, the velocity of the piston head in the static test can differ substantially from the velocity of the rocket on a piston launcher only if there are substantial and non-negligible differences in aerodynamic drag. During piston travel, the duration for which velocity is substantial (say, greater than 10m/sec) is typically very brief (at most 0.075 second for A motors). If we assume a 10mm piston head has an average velocity of $15m/sec^2$ lasting 0.075 second, and further assume a fixed drag coefficient of 1.0, the sum of the aerodynamic drag during this period would be

$$\int D^*_{Aero}(t) = (0.075)\ (0.5)\ (1.225kg/m^3)\ (15m/sec)^2\ (0.005)^2\ \pi = 0.0008N\text{-}sec.$$

This calculation makes it clear that the aerodynamic drag of the static test is negligible. We might reasonably assume the aerodynamic drag of the piston-launched rocket is higher, but even with a 12-fold increase, the sum of this drag would still have less than 0.01N-sec of impact. So we feel it is reasonable to assume $D^*_{Aero}(t) = D_{Aero}(t) = 0$ and that $a^*(t) = a(t) = 0$. These assumptions allow us to simplify the formula for $F^*(t)$:

$$F^*(t) = F(t) = (9.82\ m/sec^2)^{-1}\ W\ a(t) + W.$$

In the current study, we applied the same definition of piston-adjusted thrust, but made two key changes to the static testing and data collection scheme. First, the clear plastic tube was replaced with a conventional Kraft paper tube, as would be typical of an actual piston launch. Second, we measured the upward thrust $F^*(t)$ against the movable piston head by directly measuring the downward thrust of the motor and tube against an aluminum plate (rigged to a load cell and data acquisition system, described in more detail in Section 5). These changes greatly increased the accuracy of the static test data and the relevance to "real world" piston launches of rockets.

The acceleration during piston travel is directly obtained as

$$a(t) = (9.82\ m/sec^2)\ W^{-1}\ [F(t) - W]\ .$$

For each static test, the data acquisition system provided 240 samples per second, or roughly 15 to 40 samples of F(t) during piston travel. So for each discrete time point, we derived the length of piston travel L(t) as an iterative function of the acceleration a(t):

$L(t_0) = L_0$ (where L_0 = starting length used for the initial volume).

$L(t_1) = (t_1 - t_0)^2\ a(t_1) + L_0\ .$

For $i > 1$, $L(t_i) = L(t_{i-1}) + (t_i - t_{i-1})^2\ a(t_i) + \big(L(t_{i-1}) - L(t_{i-2})\big)\ (t_i - t_{i-1}) / (t_{i-1} - t_{i-2})$.

The cumulative impulse C(t) up to time t, associated with the length of travel L(t), was also calculated iteratively:

$C(t_0) = 0$

For $i > 0$, $C(t_i) = C(t_{i-1}) + (t_i - t_{i-1})\ F(t_{i-1}) + 0.5\ (t_i - t_{i-1})\ [F(t_i) - F(t_{i-1})]$.

For each type of motor being used in the study, we first performed a conventional static test measuring M(t) using the same load cell with same calibration as the piston tests. The motor's impulse $C_M(t)$ was calculated for each time t as described above. For each motor/piston configuration tested, we similarly calculated the impulse $C_F(t)$, so that we were able to directly measure the difference in impulse $C_F(t) - C_M(t)$ at every time point. From these discrete measurements, we could also interpolate the increased impulse at any time point and length of travel that falls in between the observed values.

The impulse is maximized at the time point t and the associated length of travel L(t) where $C_F(t) - C_M(t)$ is maximized. This corresponds to the length of travel where ideally the rocket should separate from the piston, where no further increase in impulse (over that of the unassisted motor) will be gained from additional piston travel.

Note that our definition of piston-adjusted thrust does not apply to the "coasting" portion of a floating-head piston launch (where the piston tube is no longer in relative motion to the piston head). Nor does it apply to the instantaneous effect of a model's separation from a piston tube. We assume that neither of these factors substantially adds to the motor's unassisted thrust. It is likely that the jolt of a model's separation from a piston tube will momentarily reduce acceleration (and possibly reduce velocity) regardless of whether a fixed or floating head piston launcher is used. This reduction may be less severe for floating head pistons. However, the coasting portion of a floating head launch (where the motor and piston are in a closed configuration with no relative motion between the tube and head) is unlikely to provide as much thrust as the motor would burning in the open air (considering, for example, the Krushnik effect). Given the tradeoffs, we see no particular performance advantage to the floating head design, other than possibly reducing the number of tipoffs at separation. Either design, when executed well, should provide similar performance. In any case, the methods of the current study for identifying optimal length should be applicable to either type of launcher. This topic was discussed in greater detail in our NARAM-55 report, so we refer the interested reader to that more expanded discussion.

(5) Test Methods and Materials (with Budget)

Table 1 below lists all the equipment and materials that were used in the current study. Approximate costs are indicated only for non-reusable materials. The 10mm motors used in the study were donated, and therefore costs of these motors are not listed. The total budget (the sum of the indicated costs) was approximately $124.

Table 1

Materials and Equipment	**Approximate Cost, $**
12 Estes A3 motors (A012808) 6 Ultra A2 motors (matching label and date 08-2010) 4 Apogee A2 motors (matching date April 24, 1996) Estes Solar Igniters	30
34-inch Kraft paper tubing (10mm and 13mm)	75
Brass tubing, Mylar tape, ballast (for piston heads)	16
5-minute epoxy	3
12V battery, ignition system Aerocon 10kg load cell and thrust plate DataQ DI-145 Data Acquisition (DAQ) module Microsoft Excel, Word; DataQ WinDAQ software: on HP Elitebook & Apple Macbook Air laptop computers	
Total	124

The photograph on the next page shows the Aerocon thrust plate used in all of our tests. One end of the load cell is attached underneath the top thrust plate, while the other end of the load cell is attached to the base at the bottom of the unit. The 10kg load cell is most accurate in the range below 10kg (roughly below 100N). So its use for model rocketry applications is appropriate.

We performed a number of initial tests to determine the best approach to calibrating the load cell readings. The DataQ DI-145 module limited the precision of measurements to within about 10g, or roughly 0.1N. We considered various test weights between 0.1kg and 3kg, and eventually calibrated so as to maximize accuracy in the lower half of this weight range. So we ended up with accuracy within ±10g for weights up to

1.5kg, within -40g at 2.0kg, and within -90g at 2.5kg and 3.0kg. So for example, after calibrating, the 3.0kg weight read as 2913g. As indicated here, the error for the weights 2.0kg and higher was in each instance an under-estimate. This approach to calibration made the most sense, because the pistons tend to have longer periods of time generating thrust at levels below 1.5kg, whereas spikes of thrust above 1.5kg tend to be very brief. So in this way, we minimized the impact of the error on impulse calculations.

More importantly, following calibration, all test weights showed reproducibility within the ±10g resolution of the DataQ module following repeated tests and/or repeated applications of pressure to the thrust plate. This precision over time allowed for valid comparisons between different static tests, such as when measuring the increase in impulse over a previous test.

For the piston tests, our procedure was as follows:

1. Cut a 2mm carbon fiber (CF) stick to the length appropriate for the intended initial volume (if applicable for that test).
2. Fit and secured the igniter into the motor.
3. Glued the motor and CF stick (if applicable) into one end of the tube using 5-minute epoxy (the epoxy provided an air seal between the motor and piston tube). The motor was placed 1 cm inside the tube.
4. At some time after the epoxy cured, obtained the right fit for the brass piston head inside the 34-inch paper piston tube, by adding and/or removing wraps of mylar tape to achieve the best fit. A fresh layer of mylar tape on the piston head was required for each test, so that the head would fit snugly yet move smoothly within the particular tube to be used for that test.
5. Used a 6-foot, ¼-inch steel launch rod to push the 28g piston head all the way down the piston tube, until it butted up against the motor or CF stick.
6. Placed the motor end of the piston/motor unit onto the test stand and hooked up the ignition system.
7. Began recording data, then ignited the motor.

Readings from the load cell were transferred electronically, first through an amplifier, then through the DataQ DI-145 module. The DataQ module digitally sampled the amplified analog voltages at a rate of 240 samples per second, effectively

translating the voltages into discrete values for the measured thrust. The WinDAQ software running on the HP computer read in the sampled values from the DataQ module. For data analyses, the WinDAQ data was transferred into Excel. The methodology presented in Section 4 formed the framework for all further data analyses, with calculations run (and all figures created) using Excel software. Figures for thrust curves presented in this report have been "smoothed" between discrete points for easier visual interpretation; however, all calculations for acceleration, velocity, length of piston travel, and impulse were derived from the exact, sampled thrust values. So only the visual representations were smoothed by the Excel graphic function.

For all figures of thrust curves shown in this report, the vertical axis is in Newtons while the horizontal axis is in seconds. For simplicity of presentation, I have omitted these units from the figures themselves.

(6) List of All Static Tests Performed

Table 2: 22 static tests, listed in chronological order

Motor	Tube Length	Tube Diameter	Initial Volume	Test Date
Estes A3		Motor only --- No Piston		July 1, 2014
Estes A3		Motor only --- No Piston		July 1, 2014
Estes A3	86cm	13mm	Zero	July 1, 2014
Estes A3	86cm	13mm	Zero	July 1, 2014
Estes A3	86cm	13mm	$2cm^3$	July 3, 2014
Estes A3	86cm	13mm	$4cm^3$	July 3, 2014
Estes A3	86cm	13mm	$6cm^3$	July 3, 2014
Estes A3	86cm	13mm	$8cm^3$	July 3, 2014
Estes A3	86cm	13mm	$8cm^3$	July 7, 2014
Estes A3	86cm	13mm	$8cm^3$	July 9, 2014
Ultra A2	86cm	Motor only --- No Piston		July 9, 2014
Ultra A2	86cm	Motor only --- No PIston		July 9, 2014
Apogee A2	86cm	Motor only --- No Piston		July 9, 2014
Apogee A2	86cm	10mm	Zero	July 10, 2014
Apogee A2	86cm	13mm	Zero	July 10, 2014
Estes A3	86cm	10mm	Zero	July 10, 2014
Ultra A2	86cm	10mm	Zero	July 10, 2014
Ultra A2	86cm	10mm	Zero	July 10, 2014
Apogee A2	172cm	10mm	Zero	July 11, 2014
Estes A3	172cm	10mm	Zero	July 11, 2014
Ultra A2	172cm	10mm	Zero	July 11, 2014
Ultra A2	172cm	10mm	Zero	July 11, 2014

(7) Motor Thrust Curves

In this section, we present data from our own static tests of the motors, without pistons. All static tests for motors and pistons were conducted using the same load cell under the same calibration as discussed in Section 5.

We measured the thrust-time curve M(t) for two Estes A3-4T motors from our set of test motors. In Figure 1, we show the first motor's curve, the one used for all subsequent analysis and comparison with the A3 piston-adjusted thrust curves.

Figure 1: Estes A3-4T Motor Thrust-Time Curve M(t)

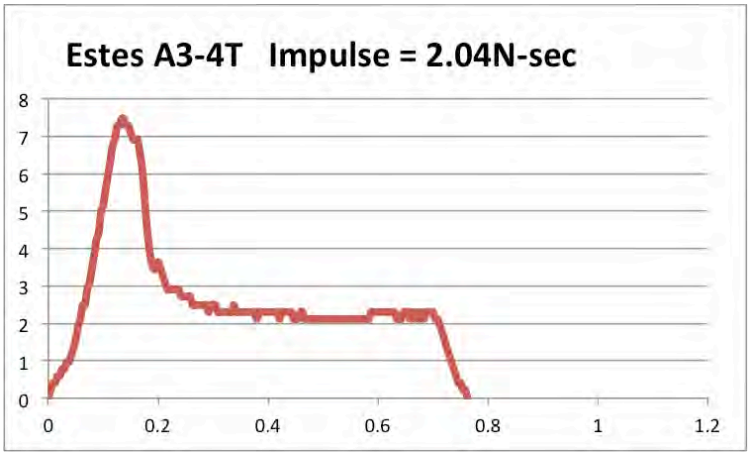

The second motor tested showed great similarity to the first, differing in impulse by only 0.01N-sec. Figure 2 shows the graphs for both motors together.

Figure 2: Two Estes A3-4T Thrust-Time Curves

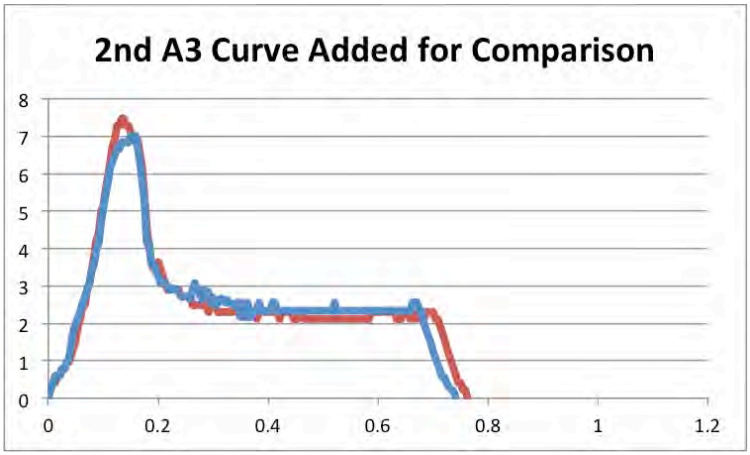

More importantly, the two A3 motors showed remarkable consistency during the first 0.1 second (Figure 3) when the piston is in motion. During this brief moment of thrust, impulse differed by just 0.004N-sec. The similar impulse and pattern during the first 0.1 second of the thrust curve indicated that our use of A3 motors with matching serial numbers did provide sufficient control of between-motor variation.

Figure 3: Estes A3 --- 1st 0.1 Second of Thrust

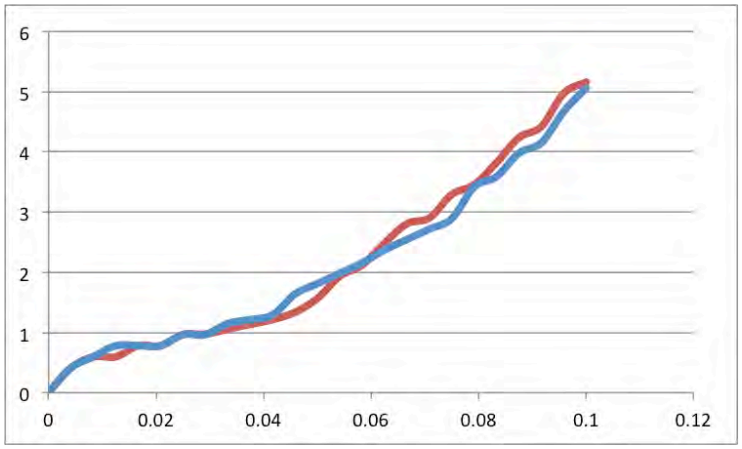

Impulse = 0.210 N-sec

Impulse = 0.206 N-sec

Figure 4 at the top of the next page shows the motor thrust curve M(t) for the first Ultra A2 motor tested, while Figure 5 adds to Figure 4 the thrust curve of a second Ultra A2. These two Ultra A2 motors differed in impulse by only 0.008N-sec.

Figure 6 at the bottom of the next page shows the first 0.15 second of each Ultra A2 thrust curve (The Ultra tended to have slower piston travel than either the Estes or Apogee). Impulse differed by just 0.006N-sec (0.363N-sec versus 0.357N-sec) during this part of the thrust curve relevant to piston performance. More importantly, the pattern of the thrust curve is very similar between the two Ultra motors. As with the A3 motors, our results for the two Ultra motors support an assumption of adequate control of variability between Ultra motors.

Figure 4: Ultra A2 Motor Thrust-Time Curve M(t)

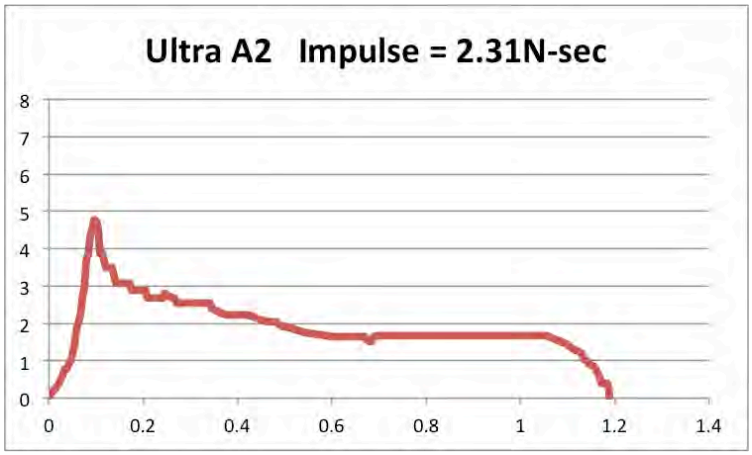

Figure 5: Two Ultra A2 Thrust-Time Curves

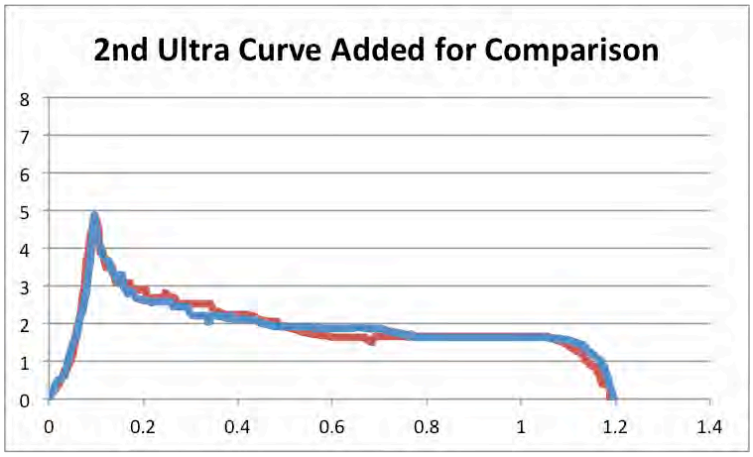

Figure 6: Ultra A2 --- 1st 0.15 Second of Thrust

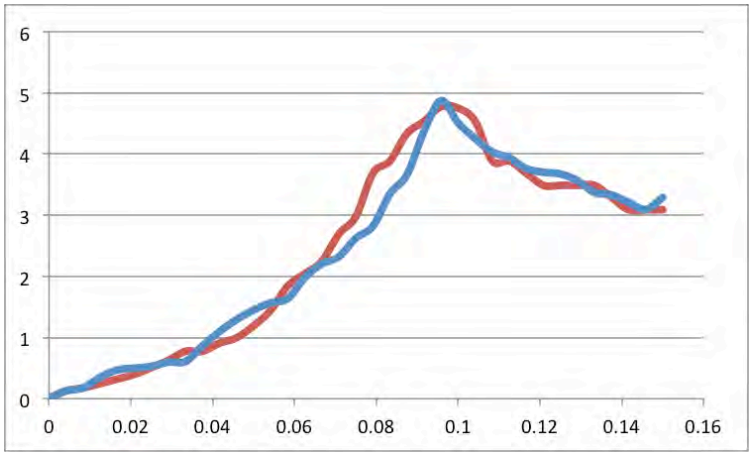

The Apogee A2 was tested only once without a piston. Figure 7 below shows the full motor thrust curve M(t). The Apogee performed the closest among the three types of motors to published thrust curves, remarkable for a motor nearly 20 years old.

Figure 7: Apogee A2 Motor Thrust-Time Curve M(t)

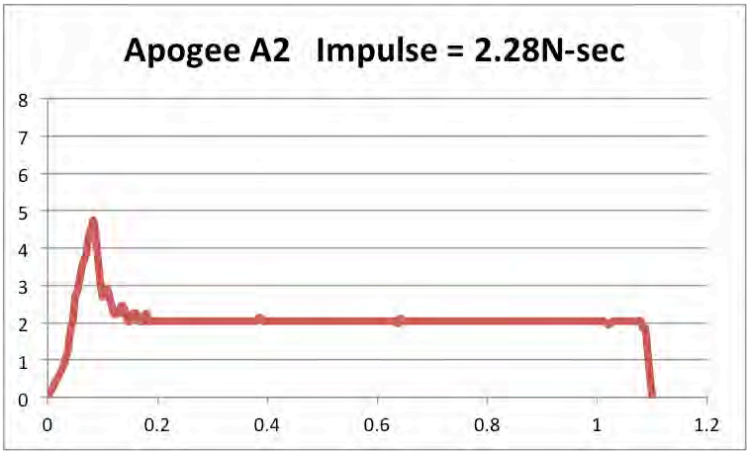

Results in the next section will show how piston-adjusted thrust differed for the three types of motors. When controlling for factors other than the type of motor, the observed differences in the pattern of piston-adjusted thrust are most likely the result of differences in the shape of the early part of the thrust curve. For example, the first spike in thrust occurs within 0.02 or 0.03 second. Figure 8 below shows how the three types of motors differ during just the first 0.025 second.

Figure 8: Differences in Motor Thrust During the 1st 0.025 Second

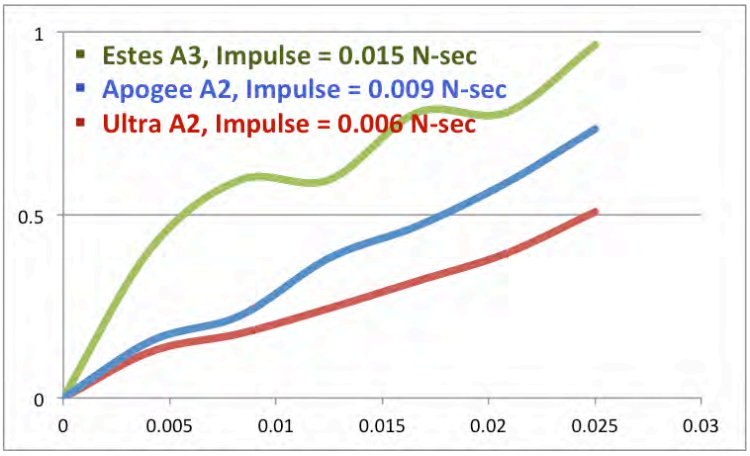

As clear from Figure 8, the Estes A3 is the strongest motor during the first 0.025 second, with the Ultra motor the weakest. So we expect the initial piston-adjusted thrust spike from the Estes motor to be the highest, that of the Ultra to be lowest. However, for longer pistons the overall piston-adjusted impulse should be higher for the Apogee A2, because after about 0.03 second, the Apogee A2 surpasses the Estes A3 and clearly dominates the other motors between 0.04 and 0.075 second (Figure 9). At 0.075 second, the A3 has about 33% more impulse than the Ultra A2, while the Apogee A2 has about 25% more impulse than the Estes A3.

Figure 9: Differences in Motor Thrust During the 1st 0.075 Second

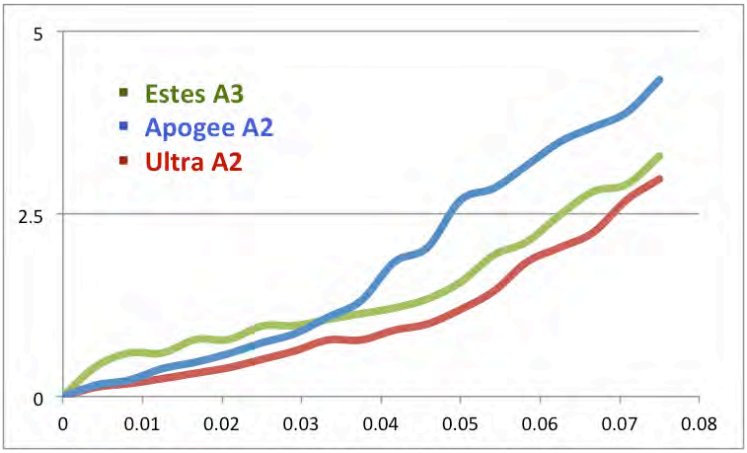

Apogee Impulse = 0.132 N-sec

Estes Impulse = 0.105 N-sec

Ultra Impulse = 0.078 N-sec

It is important to recognize that the relationship between the motor's thrust and the piston-adjusted thrust will depend on the particular volume of the piston at each point in time. As we show in the next section, a piston can provide a nearly 30-fold magnification of impulse within the first 0.025 second after ignition. At say, 0.05 second after ignition, the motor's thrust may be several times greater, but by then the piston volume has already expanded so much that the piston-adjusted thrust may wane or oscillate. So while there is likely to be some general relationship between motor thrust and piston-adjusted thrust, this relationship is dynamic and complex.

(8) Piston-Adjusted Thrust Curves and Optimal Configurations

We will present results roughly following the chronological order in which tests were done (See Table 2 in Section 6).

Figure 10 below shows the piston-adjusted thrust curve for the Estes A3 in an 86cm tube with 13mm diameter and zero initial volume. Table 3 at the top of page 25 shows the same piston-adjusted thrust data linked to derivations of velocity, length of travel, and impulse. A second test of the A3 motor under the same settings yielded a very similar thrust curve and an identical optimal configuration (data not shown).

A study of Table 3 shows that the highest observed increase in impulse over that of the motor occurred at 30.8cm. However, because the thrust at 30.8cm is negative, we know the increase in impulse was actually optimized at a length of travel in between 24.2cm and 30.8cm. By interpolating, we calculated that the piston-adjusted thrust would have fallen to match the motor's thrust at a length of travel of 29.4cm. This is the length at which the rocket should separate from the piston, where the increase in impulse over that of the motor is maximized. So for a 13mm piston with zero initial volume, the optimal length of travel is 29.4cm. The increase in impulse is 0.44N-sec, or about a 22% increase over the A3 motor's measured impulse of 2.04N-sec.

Figure 10: Estes A3, Piston-Adjusted Thrust During 85cm of Travel
13mm Diameter, Zero Volume

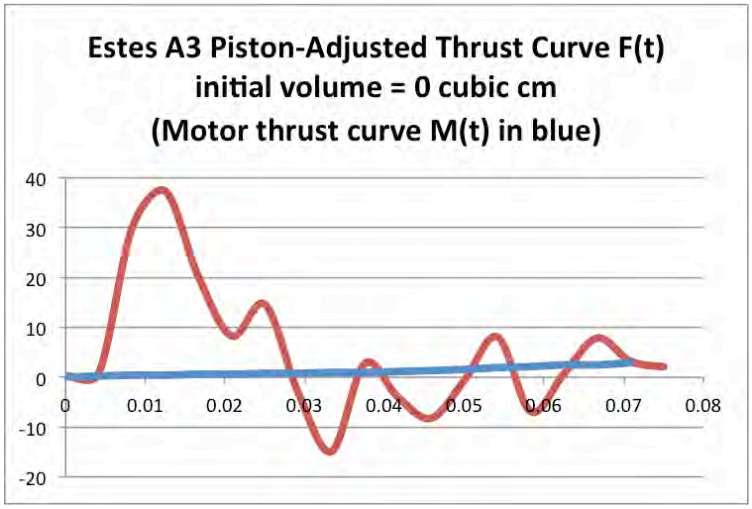

Table 3: Velocity, Thrust, and Impulse by Length of Travel (up to 85cm) Estes A3 using 13mm Diameter, Zero Volume

Time, sec	Length of Travel, cm	Velocity, m/sec	Piston-Adjusted Thrust F(t), N	Piston-Adjusted Impulse, N-sec	Increased Impulse over the Motor, N-sec
0	0	0	0.275	0	0
0.0042	0	0.10	0.917	0.002	0.002
0.0083	1.9	4.51	29.961	0.067	0.065
0.0125	6.1	10.03	37.328	0.207	0.203
0.0167	11.5	12.98	20.118	0.327	0.321
0.0208	17.4	14.17	8.285	0.386	0.378
0.0250	24.2	16.30	14.578	0.433	0.422
0.0292	30.8	15.80	-3.0629	0.457	0.443
0.0333	36.4	13.55	-14.895	0.420	0.402
0.0375	42.2	13.91	2.746	0.395	0.373
0.0417	47.8	13.28	-3.977	0.392	0.366
0.0458	52.8	12.02	-8.226	0.367	0.335
0.0500	57.7	11.88	-0.643	0.348	0.311
0.0542	63.2	13.04	8.070	0.364	0.319
0.0583	68.1	11.98	-6.881	0.366	0.313
0.0625	73.2	12.04	0.702	0.353	0.291
0.0667	78.6	13.17	7.855	0.371	0.298
0.0708	84.2	13.60	3.211	0.394	0.310
0.0750	Exit	13.87	2.100	0.405	N/A

The periods of negative thrust (deceleration) observed for the A3 were surprising to us, but we are convinced these observations are real. At first, we were tempted to think the negative thrust readings were an artifact of errant vibrations in the test stand, but an investigation convinced us that there was no way to produce such negative readings of this magnitude and clarity simply by rapidly or repeatedly applying pressure to the test stand. Furthermore, for each of our tests, the time point at which we calculated the piston head exiting the test tube is associated with a substantial drop in thrust. This provides strong evidence of the accuracy of the thrust readings; if our thrust readings were in any substantial way inaccurate (such as erroneously reading negative values), there is no way the length of travel (calculated directly from the thrust) could so accurately identify the moment of exit across all of our tests.

Figure 10 is consistent with previous observations (noted in Section 3) of cycles, or oscillations in piston-adjusted thrust. However, to our knowledge, this is the first confirmation of this pattern for the A3 motor. The thrust curve in Figure 10 is also consistent with the theory that a severe drop in piston thrust tends to follow the very large initial thrust spike associated with zero initial volume. This result led us to investigate whether the use of non-zero initial volume might sufficiently dampen the initial thrust spike, thereby avoiding the severe drop in thrust, and ultimately obtaining greater impulse via a more extended period of substantial piston-generated thrust.

Figure 11 below shows the piston-adjusted thrust curves for three values of initial volume (0, 2, and 4 cubic cm). At these values of initial volume, the general pattern of the piston-adjusted thrust curve remains the same, with no improvement in impulse nor any change in the optimal length. However, we do see evidence in Figure 11 that increasing the initial volume does dampen the thrust spike. Also, there is a pattern evident in Figure 11 that non-zero initial volume tends to delay the thrust spike, with slightly greater delay as the initial volume increases.

Figure 11: Estes A3, Piston-Adjusted Thrust, 13mm diameter, 86cm tubes

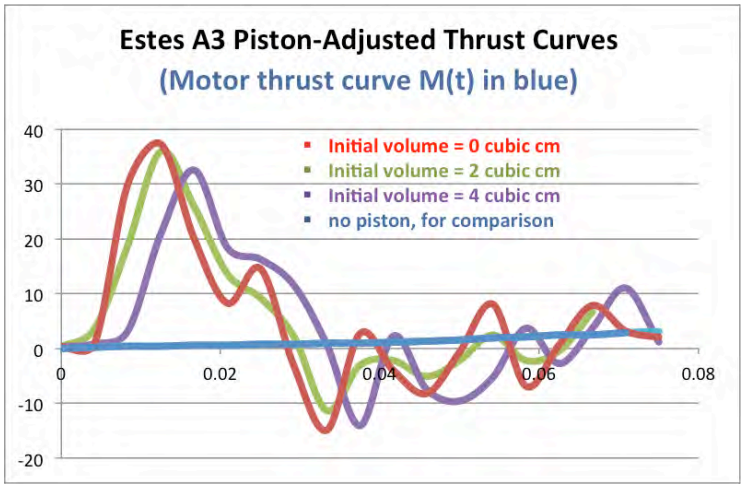

Figure 12 on the next page shows the effect of larger initial volumes. At each increase in the initial volume, we observed the thrust spike to decrease in magnitude. By 8cm^3, we now see evidence of the more desirable thrust curve we seek: The initial thrust spike is reduced enough so that a second, substantial thrust spike follows it. So by

expanding the initial volume to 8cm^3, we have fundamentally changed the pattern of the piston-adjusted thrust curve. Figures 11 and 12 provide confirmation that our theory about initial volume is essentially correct: For a given motor, there will be some quantity of initial volume that dampens the immediate thrust spike sufficiently so as to reduce the severity of the drop in thrust that follows the spike. However, it may not always be the case that the configuration with non-zero initial volume leads to a substantially higher increase in impulse.

Figure 12: Estes A3, Piston-Adjusted Thrust, 13mm diameter, 86cm tubes

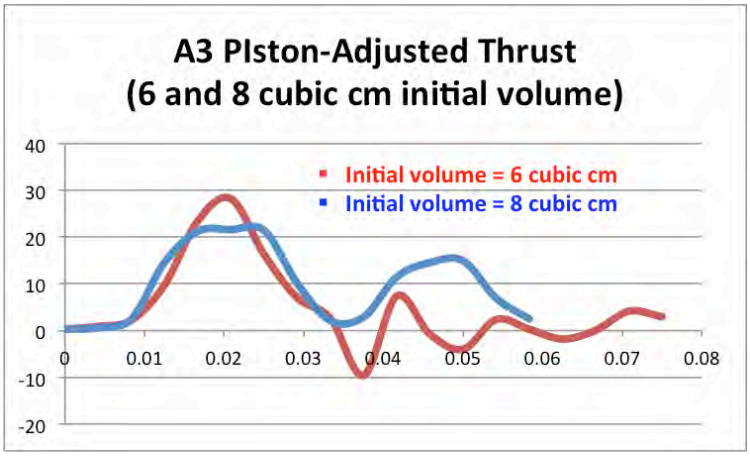

To confirm the result at 8cm^3, we conducted two additional tests at this same initial volume, with all other factors the same. Figure 13 at the top of the next page shows the thrust curves for all three of the tests at 8cm^3. All three tests show the same general pattern of piston-adjusted thrust, each different from the pattern typical of the smaller initial volumes. However, the two additional tests showed somewhat lower impulse than that observed for the first test at 8cm^3. Table 4 summarizes the data with piston-adjusted thrusts averaged across the three tests so as to provide an unbiased evaluation of this particular piston configuration. The optimal length of travel is 69.5cm (including the 6cm "head start" due to the initial volume). The increased impulse for this configuration is 0.48N-sec over that of the unassisted motor. This represents a small improvement (on average) over the optimal length of travel of 29.4cm at zero volume, which increased the motor's impulse by 0.44N-sec. The weight of the additional 40cm of tubing amounts to only 0.003N-sec of opposing impulse with this configuration, so the 0.04N-sec improvement in piston-adjusted thrust is not trivial.

Figure 13: Estes A3 with 8cm^3 Initial Volume: Results for 3 (Replicated) Tests

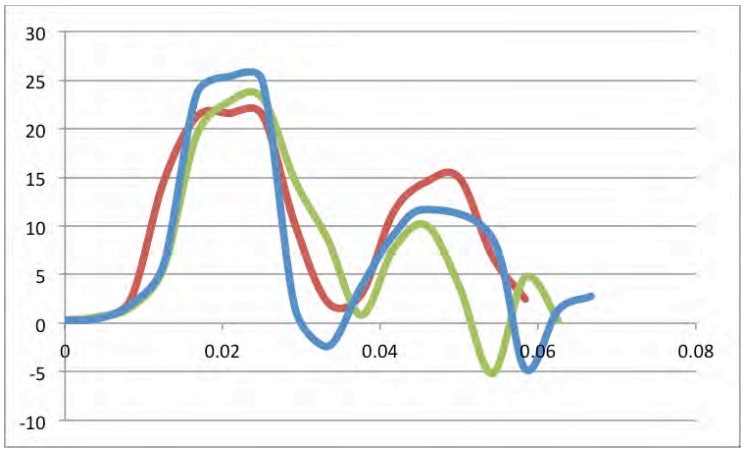

Table 4: Velocity, Thrust, and Impulse by Length of Travel Estes A3, 13mm Diameter, 86cm tube, 8cm^3 Initial Volume

Time, sec	Length of Travel, cm	Velocity, m/sec	Piston-Adjusted Thrust F(t), N	Piston-Adjusted Impulse, N-sec	Increased Impulse over the Motor, N-sec
0	6	0	0.275	0	0
0.0042	6	0.04	0.573	0.002	0.001
0.0083	6.1	0.30	2.014	0.007	0.005
0.0125	6.8	1.57	8.779	0.030	0.026
0.0167	8.6	4.71	21.357	0.092	0.087
0.0208	12.1	8.13	23.258	0.185	0.177
0.0250	17.0	11.54	23.188	0.282	0.271
0.0292	22.3	12.80	8.770	0.349	0.334
0.0333	27.8	13.17	2.757	0.373	0.355
0.0375	33.4	13.50	2.472	0.384	0.362
0.0417	39.6	14.86	9.414	0.408	0.382
0.0458	46.5	16.62	12.104	0.453	0.422
0.0500	54.0	17.96	9.328	0.498	0.460
0.0542	61.7	18.44	3.505	0.525	0.479
0.0583	69.5	18.73	2.122	0.536	0.483
0.0625	77.0	18.36	-0.824	0.539	0.476

We also shot video for the test of the A3 with 4cm^3 initial volume, using the high-definition, 120 frames-per-second camera on the iPhone 5S. This particular test was chosen arbitrarily; the point of the video was to get an additional confirmation that the timing of the piston head's exit from the tube was matching our derived calculation of length of travel. From the formula in Section 4, we calculated 80cm of travel 0.075 second after ignition. At this length of travel, just 5cm short of full length, the top half of the roughly 10cm-long brass piston tube should have been visible, emerging from the top of the piston tube. From the video, we were able to identify the moment of ignition and the moment the top of brass piston emerged from the tube, exactly 9 video frames after ignition. Nine frames of this video represents exactly 0.075 seconds. So we got a perfect match between the duration of piston travel measured by video and that same duration measured according to the methodology of Section 4. This not only verified our formula for length as correct, but also verified our assumption of negligible drag for the piston head. More importantly, this video provided verification that our load cell was measuring piston-adjusted thrust accurately. If there were substantial bias in the thrust measured by the load cell, then our derived calculations of length would be biased and would not match up so well with the video.

One test of the Apogee A2 motor involved adapting this 10mm motor to a 13mm piston tube, to see the effect of using a larger diameter piston tube. The performance was later shown to be very poor (roughly 33% of the impulse) compared to the performance of this motor in a 10mm-diameter piston. This confirmed our expectation that increasing diameter greater than the motor's diameter detracts from piston performance. Details of this test are omitted here, and no further tests increasing diameter were performed.

Figures 14-16 on the next page show piston-adjusted thrust at zero volume in 10mm-diameter, 86cm tubes. These results were surprising in that all three show benefit to using the entire length of piston tube. The pattern of piston-adjusted thrust differs substantially for each type of motor, but these results are consistent with the early motor thrusts we observed in Figures 8 and 9 presented in Section 7. Very distinct from the 13mm tests, none of the tests with 10mm-diameter pistons showed any negative values for thrust. The 10mm diameter appears to allow for more sustained piston pressure without severe drops in that pressure.

Figure 14: Ultra A2, Piston-Adjusted Thrust Curve
10mm diameter, Zero Volume, 86cm-long Tube

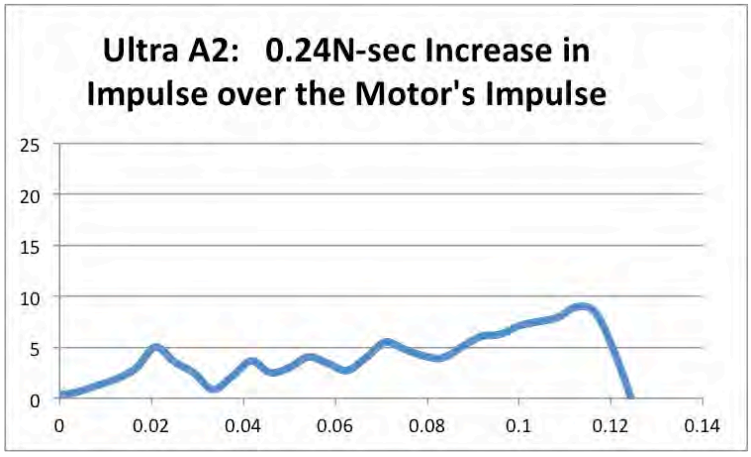

Figure 15: Apogee A2, Piston-Adjusted Thrust Curve
10mm diameter, Zero Volume, 86cm-long Tube

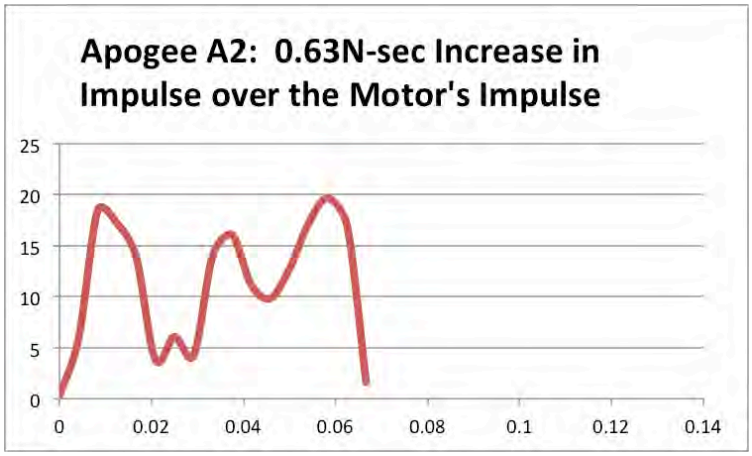

Figure 16: Estes A3, Piston-Adjusted Thrust Curve
10mm diameter, Zero Volume, 86cm-long Tube

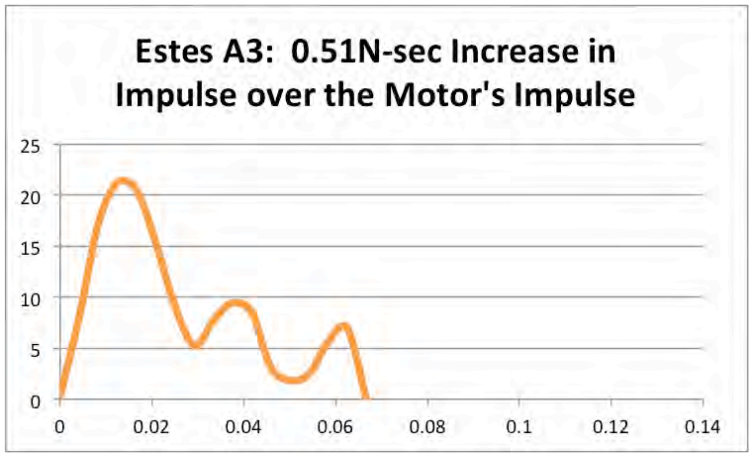

For each of these tests with 10mm-diameter pistons, the piston-adjusted thrust was over 5N at the time the piston heads exited the tubes. This suggested that substantial additional benefit was possible with still longer piston tubes. So we proceeded to run additional tests at 10mm using two-piece, 172cm piston tubes. Figures 18-20 on the next page show the piston-adjusted thrust curves when using the 172cm tubes.

Results in Figures 18 and 19 show that both A2 motors benefit from the full 172cm of piston tube length.

However, the A3 piston-adjusted thrust (Figure 20) wanes as the piston head entered the second piece of tubing; the point where the piston-adjusted thrust curve crosses the A3 motor thrust curve corresponds to 91cm of piston travel. So the optimal length of travel for the A3 motor when using a 10mm-diameter piston is 91cm, with a 0.54N-sec increase in impulse over that of the motor. However, just a single full-length tube (85cm of travel) showed a 0.53N-sec increase in impulse over that of the motor. So most modelers will no doubt find it convenient to use the single 86cm tube.

Figure 17 below shows the great consistency between the two piston-adjusted thrust curves for the A3 motor in the 10mm-diameter pistons. The average increase in impulse between the two tests (at 85cm of travel) is 0.52N-sec. This is the optimal piston configuration we found for the Estes A3 motor.

Figure 17: Estes A3, Two Piston-Adjusted Thrust Curves
10mm Diameter, Zero Volume, 85cm of travel
(one test with 86cm tube and one test with 172cm tube)

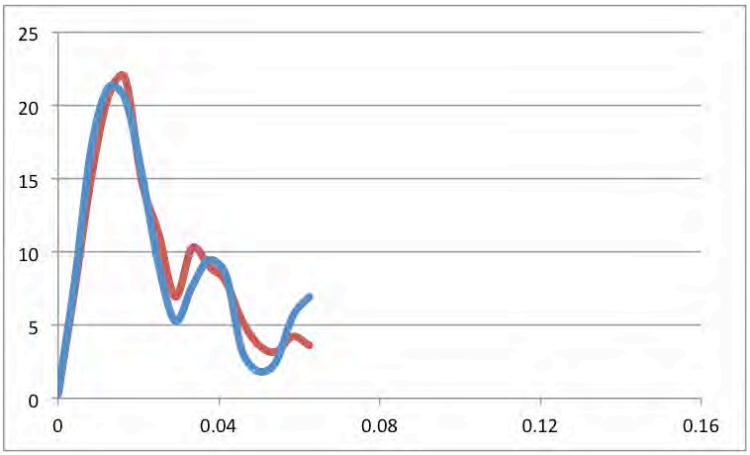

Figure 18: Ultra A2, Piston-Adjusted Thrust Curve
10mm diameter, Zero Volume, 172cm-long Tube

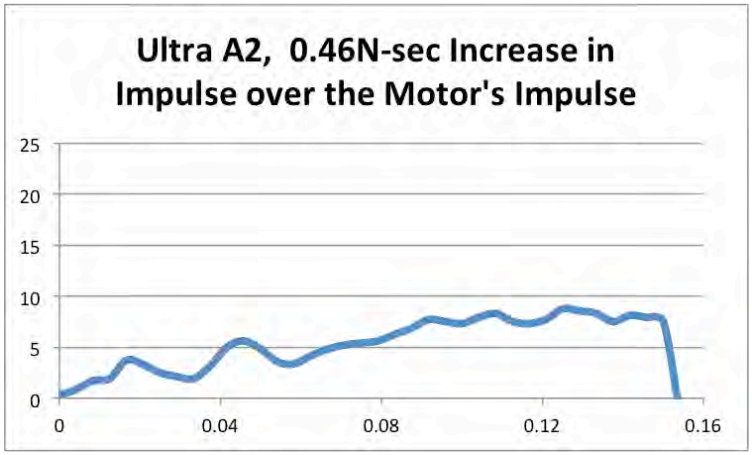

Figure 19: Apogee A2, Piston-Adjusted Thrust Curve
10mm diameter, Zero Volume, 172cm-long Tube

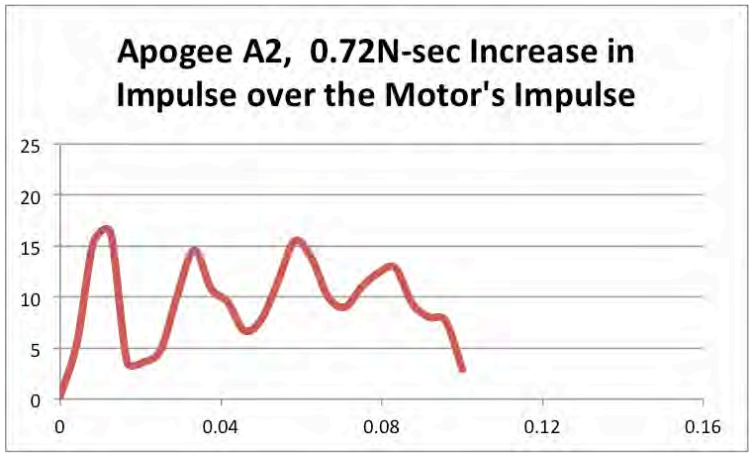

Figure 20: Estes A3, Piston-Adjusted Thrust Curve (with Motor Thrust Curve)
10mm diameter, Zero Volume, 172cm-long Tube

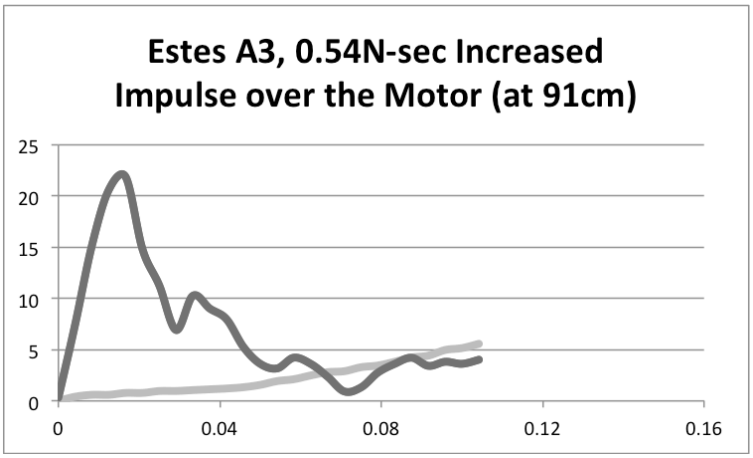

Although theoretically the Ultra and Apogee motors might show a further performance enhancement through the use of non-zero initial volume, we chose not to pursue this. In fact, the pattern of the piston-adjusted thrust curves for these motors do not show severe drops in thrust; so they do not fit the profile of a motor that might benefit from non-zero volume. The results in Figures 18 and 19 indicate sustained piston pressure over the entire 172cm of piston length --- an extraordinary result considering that it is very unlikely any modelers have ever used pistons more than half this length in FAI competition. So the optimal piston configuration for both A2 motors is a zero volume, 10mm diameter piston of length 172cm.

We did perform additional tests of the Ultra motor at both 86cm and 172cm, looking to confirm the results demonstrated by Figures 14 and 18. Figure 21 shows variability between the four tests, but nonetheless the same general increasing pattern of piston-adjusted thrust is evident. More importantly, the same optimal piston configuration was indicated by the confirmation tests, despite the noise between curves.

Figure 21: Ultra A2, Four Piston-Adjusted Thrust Curves
10mm Diameter, Zero Volume, 85cm or 171cm of travel
(two tests with 86cm tube and two tests with 172cm tube)

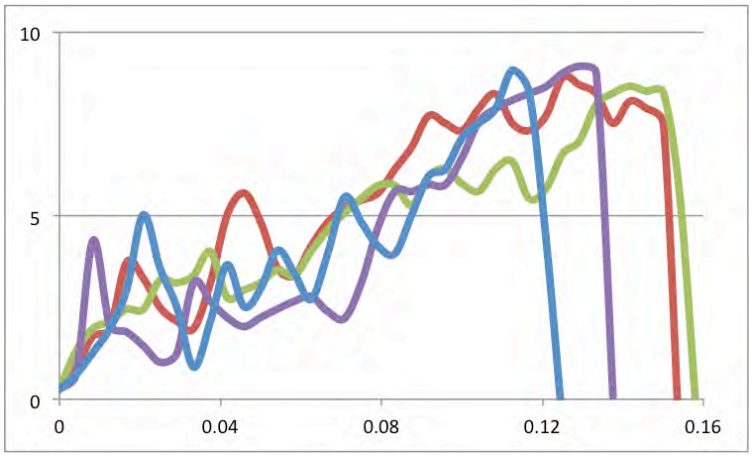

Figure 22 at the top of the next page shows the consistency of results between the two 10mm Apogee piston-adjusted thrust curves. Tables 5-7 show details of the performance at each optimal piston configuration.

Figure 22: Apogee A2, Two Piston-Adjusted Thrust Curves
10mm Diameter, Zero Volume, 85cm or 171cm of travel
(one test with 86cm tube and one test with 172cm tube)

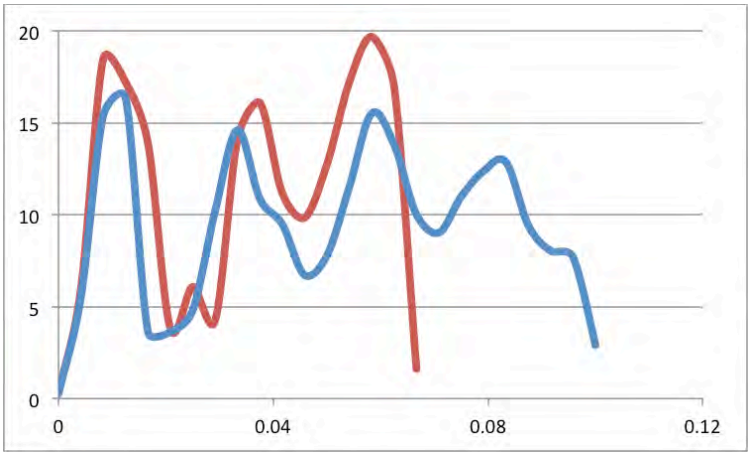

Table 5: Velocity by Length of Travel, for Selected Time Points
Ultra A2, 10mm Diameter, Zero Volume, 172cm tube
(Optimal Piston Configuration for the Ultra A2)

Time, sec	Length of Travel, cm	Velocity, m/sec	Increased Impulse over the Motor, N-sec
0	0	0	0
0.025	2.3	1.85	0.047
0.05	10.6	4.98	0.117
0.0625	18.1	6.51	0.144
0.075	28.0	8.69	0.175
0.0875	41.0	11.36	0.203
0.1	57.9	14.59	0.238
0.1125	79.0	18.01	0.284
0.125	104.3	21.43	0.335
0.1375	134.1	24.94	0.397
0.15	168.1	28.33	0.456
0.154	Exit	N/A	N/A

Table 6: Velocity by Length of Travel, for Selected Time Points Apogee A2, 10mm Diameter, Zero Volume, 172cm tube (Optimal Piston Configuration for the Apogee A2)

Time, sec	Length of Travel, cm	Velocity, m/sec	Increased Impulse over the Motor, N-sec
0	0	0	0
0.0125	3.8	5.42	0.117
0.025	11.9	7.09	0.182
0.0375	25.1	12.28	0.300
0.05	43.4	15.73	0.381
0.0625	67.9	21.68	0.503
0.075	98.6	26.03	0.586
0.0875	135.5	31.06	0.677
0.0958	162.8	33.32	0.715
0.1	Exit	N/A	N/A

Table 7: Velocity by Length of Travel, for Selected Time Points Estes A3, 10mm Diameter, Zero Volume, 86cm tube (Optimal Piston Configuration for the Estes A3)

Time, sec	Length of Travel, cm	Velocity, m/sec	Increased Impulse over the Motor, N-sec
0	0	0	0
0.0125	4.5	6.33	0.135
0.025	18.9	13.34	0.346
0.0375	38.6	17.12	0.449
0.05	62.2	19.51	0.515
0.0583	79.1	20.52	0.529
0.625	Exit	N/A	N/A

(9) Overall Conclusions

In this study we focused on applying the technique of measuring piston-adjusted thrust in the most accurate way possible, addressing the question, "What is the optimal piston to use for the FAI parachute, streamer, and helicopter events?" Our conclusions are very clear cut for the 10mm A2 motors studied: A 172cm-long, 10mm zero-volume piston is clearly optimal for these motors (within the limits of what we tested). Despite some noise with the A2 motors, there is a generally consistent increase in piston-adjusted thrust during this entire long length of piston travel. The results were replicated and thus not based solely on a single test. The magnitude of increased impulse when using this optimal configuration was 0.46N-sec for the Ultra A2 and 0.72N-sec for the Apogee A2. The superior piston-adjusted thrust with the Apogee motor appears to be the result of the Apogee motor's greater impulse during the very early part of the motor's burn, corresponding to the duration of piston travel.

For the Estes A3 motor, the optimal piston configuration is to adapt this 13mm motor to a 10mm-diameter, zero-volume piston of length 86cm. This configuration was found to increase impulse over that of the motor by 0.53N-sec. For convenience, some modelers may prefer to use a (sub-optimal) 13mm-diameter, zero-volume piston of length 30cm (which increased impulse over that of the motor by 0.44N-sec). A third option is to use a 13mm-diameter, 70cm-long piston with $8cm^3$ of initial volume (which increased impulse over that of the motor by 0.48N-sec). Although we did not find the use of non-zero initial volume to be optimal, we did see a consistent pattern with the A3 motor that confirmed our general theory about the effect of non-zero volume on piston-adjusted thrust: For a given motor, there will be some quantity of initial volume that dampens the immediate thrust spike sufficiently so as to reduce the severity of the drop in thrust that tends to follow the spike. However, this theory proved to be irrelevant to the behavior of these A motors in the 10mm pistons, where drops in thrust at zero volume did not tend to be severe.

We are excited to report results showing that a more sustained level of piston pressure is possible by reducing the diameter of the piston tube (as with the A3 motor in this study). This suggests a potential benefit to using reduced-diameter pistons more generally with other motors and weight classes, although further study of this is needed.

(10) For Future Study

There is much about piston behavior that remains poorly understood within the community of modelers and amateur rocketeers. This current report should contribute to our understanding of pistons, but further study is needed.

For example, we do not really know why the A3 motor behaved differently in the 10mm-diameter piston than in the 13mm-diameter piston. Presumably the more sustained level of piston pressure is due to the smaller volume per unit of length, but this may not provide a complete explanation. It would be interesting to examine whether more powerful motors benefit from the use of piston diameters smaller than that of the motor. The NAR community would also benefit from deeper theoretical explanations of these observed results.

The current report and our NARAM-55 report indicate that very long pistons tend to be beneficial to improving the performance of at least certain kinds of model rockets and motors. The current report is the first to document that very long pistons (≥ 86cm) can boost the performance of lightweight models. A key question is whether optimizing pistons for most motors and weight classes will always result in very long pistons; or is this benefit restricted only to certain motors or types of motors? It may be presumptuous to assume the results for A motors will apply to other motors or weight classes without further testing.

Finally, the current study does not in any way at all examine the practical issues of launching a model rocket off a piston 172cm long. There are no doubt technical challenges to executing this efficiently. Our team has some experience with flying 100cm+ pistons using rail launchers as an additional support. In this approach, the rail lugs are attached to the piston tube, not the rocket. But no doubt there are other approaches possible to flying with very long piston launchers.

(11) Appendix: Brief Summary of Our NARAM-55 R&D Entry

In our 2013 study we defined a concept of piston-adjusted thrust, sufficiently comparable to the NAR Standards and Testing concept of motor thrust, so as to allow a direct comparison of a piston-adjusted thrust-time curve with the corresponding motor thrust-time curve. We designed and executed a method of static testing for measuring piston-adjusted thrust. This method involved firing a motor inside a clear plastic tube, against movable piston head of a fixed known weight. Velocity of the piston head upward was measured visually from high-speed video, with the acceleration derived at several points in time from the measured velocities. Piston-adjusted thrust was then calculated from the values for acceleration.

This study demonstrated that a C6 motor firing inside of a piston tube, against a 153g weight, generates impulse at a level substantially greater than the rated impulse of a C6 motor without a piston. Most of the additional impulse was generated at lengths of piston tube much longer than typically used by modelers (i.e. during the period of piston travel between 86cm and 120cm). We also showed increased impulse using a small (20 cubic cm) non-zero volume in the piston, as compared to zero volume.

Finally this study hypothesized and confirmed a pattern of oscillating (or waxing and waning) thrust when motors burn inside a piston. This confirmed a pattern of piston behavior first identified by Geoff Landis in his NARAM 17 R&D report.